Inorg. Chem. **2002**, *41*, 2608–2615

Reaction of Silicate Minerals To Form Tetramethoxysilane†

Larry N. Lewis,* Florian J. Schattenmann,* Tracey M. Jordan, James C. Carnahan, William P. Flanagan, Ronald J. Wroczynski, John P. Lemmon, Joseph M. Anostario, and Michelle A. Othon

General Electric Corporate Research and Development Center, Niskayuna, New York 12309

Received September 6, 2001

Several silicon dioxide sources were used as reagents in the base-mediated reaction with dimethyl carbonate (DMC) to make tetramethoxysilane (Q′). Several commercially available diatomaceous earth materials were investigated. High throughput screening was employed to explore over 200 silicate rocks and minerals as alternative silicon dioxide sources for formation of Q′ from DMC and base. Amorphous silicon dioxide materials are effective reagents for the Q′ forming reaction. Effective silicon dioxide sources in addition to the diatomaceous earth materials include opal and various synthetic silicates (Li, Co, and Ca).

Introduction

Silicon, in the form of silica and silicates, is the second most abundant element in the earth's crust. However, the synthesis of silicones (Scheme 1) and almost all organosilicon chemistry is only accessible through elemental silicon.[1] Silicon dioxide (sand or quartz) is converted to chemical-grade elemental silicon in an energy intensive reduction process, a result of the exceptional thermodynamic stability of silica. Silicon is reacted with methyl chloride to give a mixture of methylchlorosilanes catalyzed by copper containing a variety of trace metals such as tin, zinc, and so forth. The so-called direct process for making methylchlorosilanes was first discovered at GE in 1940, Scheme 1.[1−3] The methylchlorosilanes are distilled to purify and separate the major reaction components, the most important of which is dimethyldichlorosilane. Polymerization of dimethyldichlorosilane by controlled hydrolysis results in the formation of silicone polymers. The hydrolyzate obtained from hydrolysis is cracked at high temperature in the presence of base to give cyclic-hexamethyltrisiloxane (D3). Acid- and base-catalyzed reaction of D3 in the presence of a chain stopper is the most common industrial process for production of poly(dimethylsiloxane)s (PDMS). Worldwide, the silicone industry produces about 1.3 billion pounds of the basic PDMS polymer.

Scheme 1. Industrial Process for Production of Silicones

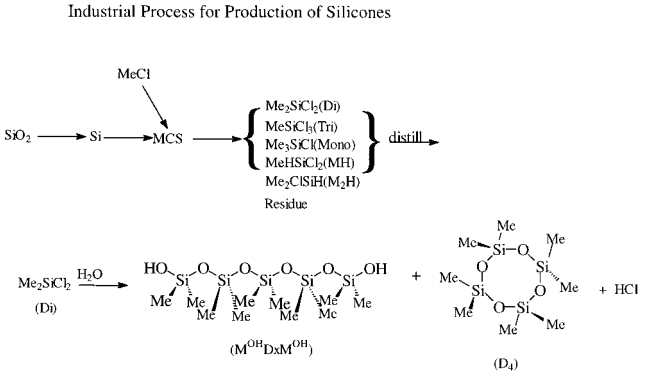

The energy costs associated with the process in Scheme 1 are mainly a result of the reduction of Si(IV) to Si(0) and subsequent reoxidation to Si(IV). The conversion of silicon dioxide to elemental silicon in an electrochemical furnace at temperatures ∼1500 °C consumes large amounts of electricity and carbon for reduction. Additionally, the production and separation of the methylchlorosilane mixture is energy intensive, involving several distillation steps. The difference in boiling points between the two main products from the direct process, dimethyldichlorosilane and methyltrichlorosilane, is 4 °C.

An alternative synthetic route to the direct process is shown in Scheme 2 where the reduction and reoxidation of silicon is avoided. The process in Scheme 2 makes alkoxysilanes instead of chlorosilanes. An alkoxysilane process has the

* Authors to whom correspondence should be addressed. E-mail: lewisln@crd.ge.com (L.N.L.); schattenman@crd.ge.com (F.J.S.).

† This work was supported by the Department of Energy Contract DC-FC02-98CH10931.

(1) *Kirk-Othmer Encyclopedia of Chemical Technology*, 3rd ed.; Wiley-Interscience: New York, 1979; Vol. 20, pp 750−880.
(2) Liebhafsky, H. A. *Silicones Under the Monogram*; John Wiley and Sons: New York, 1978.
(3) Warwick, E. L. *Forty Years of Firsts*; McGraw-Hill: New York, 1990.

10.1021/ic0109546 CCC: $22.00
Published on Web 04/10/2002

Scheme 2

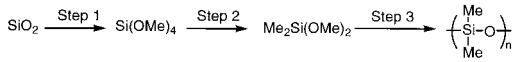

advantage of avoiding chlorine use, and the products are formed with a larger difference in boiling point than the conventional direct process; the difference in boiling point between dimethyldimethoxysilane and methyltrimethoxysilane is 20 °C.[4]

Precedence for step 1 in Scheme 2 was recently reported by Ono et al.[5] starting from silica gel and gaseous dimethyl carbonate (DMC) at 227−327 °C to yield tetramethoxysilane in the presence of a catalyst supported on the silica. The employed catalysts include MOH (M = Na, K, Rb, Cs), CsF, KF, KCl, NaCl. Rice hull ash (92% SiO_2 purity) also reacts with DMC when loaded with 5 wt % of potassium hydroxide at 352 °C.[6]

Earlier examples of the base-catalyzed activation of SiO_2 using alcohol derivatives include the formation of hexacoordinated dianionic complexes from silica (eq 1).[7]

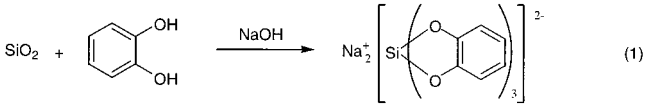

(1)

Additionally, Laine and co-workers have shown that silicon dioxide reacts with base and a diol to form a reactive pentacoordinate silicate species (eq 2); [8,9] catalyzed dissolution of SiO_2 has been reported as well.[10]

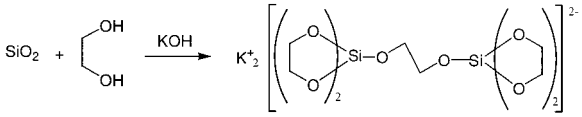

(2)

Very few other examples of the conversion of silicon dioxide to silicate-like compounds have been reported.[11−13]

Currently, the only access to dialkyldialkoxysilane from tetraalkoxysilane (step 2) involves the stoichiometric transformation using Grignard reagents.[14,15] The hydrolytic polymerization of alkylalkoxysilanes to silicone polymers (step 3) is a process that is practiced commercially.

The two major challenges connected with this proposed approach to silicones from silicon dioxide are optimization of the alkoxysilane synthesis from a low-cost silicon dioxide source and innovation of a new process for synthesis of alkylalkoxysilane from alkoxysilane. In order for the aforementioned processes to be economically viable, a low cost silicon source is required. There are hundreds of silicate minerals that could serve as potential sources of silicon dioxide. High throughput screening was used to find suitable silicate sources for formation of Q′. No other reasonable approach would permit identification of the most economical and reactive silicon dioxide source.

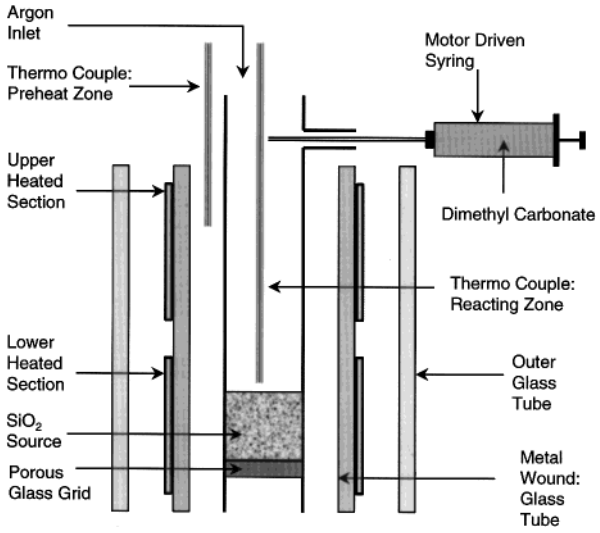

Figure 1. Schematic representation of fixed-bed flow reactor.

Experimental Section

Fixed-Bed Lab Reactor. A schematic representation of the fixed-bed flow reactor used is shown in Figure 1. The reactor was a glass tube (20 cm long, 1 cm inner diameter) with a porous glass grid to hold the SiO_2 sample. The reactor was centered vertically in a Nichrome ribbon wound glass tube (5 cm outer diameter). Two pairs of electrodes were fitted to the Nichrome to create two heated zones. The top heating zone was used to preheat the DMC/carrier gas mixture, the bottom section for the reactor itself. The Nichrome wound tube was centered in a quartz glass tube (6.4 cm outer diameter) for insulation and safety purposes. The carrier gas stream was regulated using a mass flow controller (MKS Instruments type 1179A) connected to a four-channel readout device (MKS Instruments type 247D). The DMC was added into the carrier gas stream (typically argon) above the upper heating zone through a septum via motor driven syringe. The reactor products downstream were collected using a water-chilled condenser.

Reaction of SiO_2 Source with DMC. Typical Procedure. The SiO_2 source was stirred in an aqueous solution of KOH. The suspension was heated to dryness, and the solid obtained was further dried overnight at 115 °C. The material was ground and charged into the described fixed-bed flow reactor with vertical furnace. The solid (typically 0.8 g) was kept at the reaction temperature (typically 320 °C) in the argon stream for 1 h. DMC (typically 20 mmol/h = 1.68 mL/h; a total of 10 mL) was fed into the carrier gas stream (20 mL/min) using a motor driven syringe. The reactor products downstream were collected in fractions using a water chilled condenser and analyzed by gas chromatography. Formation of $Si(OMe)_4$ was confirmed by GC/MS. The SiO_2 utilization values (%) were calculated from the collected amounts of $Si(OMe)_4$. The

(4) Source: Gelest Catalogue.
(5) Ono, Y.; Akiyama, M.; Suzuki, E. *Chem. Mater.* **1993**, *5*, 442.
(6) Akiyama, M.; Suzuki, E.; Ono Y. *Inorg. Chim. Acta* **1993**, *207*, 259.
(7) Rosenheim, A.; Raibmann, B.; Schendel, G. *Z. Anorg. Allg. Chem.* **1931**, *196*, 160.
(8) Laine, R. M.; Blohowiak, K. Y.; Robinson, T. R.; Hoppe, M. L.; Nardi, P.; Kampf, J.; Uhm, J. *Nature* **1991**, *353*, 642.
(9) Blohowiak, K. Y.; Treadwell, D. R.; Mueller, B. L.; Hoppe, M. L.; Jouppi, S.; Kansal, P.; Chew, K. W.; Scotto, C. L. S.; Babonneau, F.; Kampf, J.; Laine, R. M. *Chem. Mater.* **1994**, *6*, 2177.
(10) Cheng, H.; Tamaki, R.; Laine, R. L.; Babonneau, F.; Chujo, Y.; Treadwell, D. R. *J. Am. Chem. Soc.* **2000**, *122*, 10063.
(11) Goodwin, G. B.; Kenney, M. E. *Polym. Prepr. (Am. Chem. Soc., Div. Polym. Chem.)* **1986**, *27*, 107.
(12) Bailey, D. L. U.S. Patent 2,881,198, 1959.
(13) Kinrade, S. D.; Del Nin, J. W.; Schach, A. S.; Sloan, T. A.; Wilson, K. L.; Knight, C. T. G. *Science* **1999**, *285*, 1542.
(14) Graefe, J.; Uzick, W.; Weinberg, U. German Patent DE 3821483; *Chem. Abstr.* 112: 217263.
(15) Goodwin, G. B.; Kenney, M. E. *Adv. Chem. Ser.* **1990**, *224*, 251.

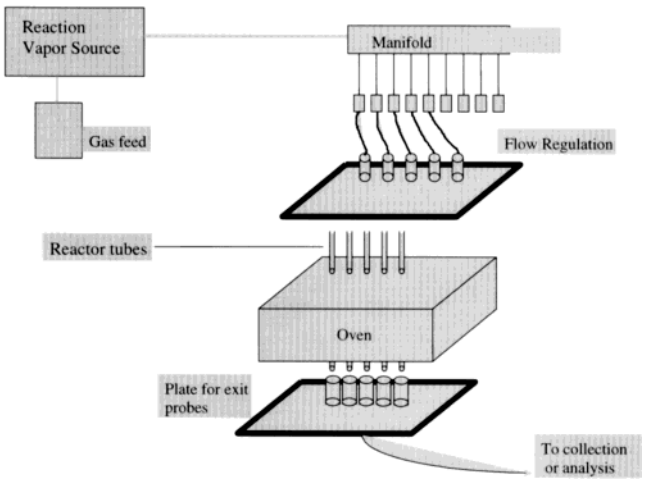

Figure 2. Block diagram of 32 tube high throughput screening reactor.

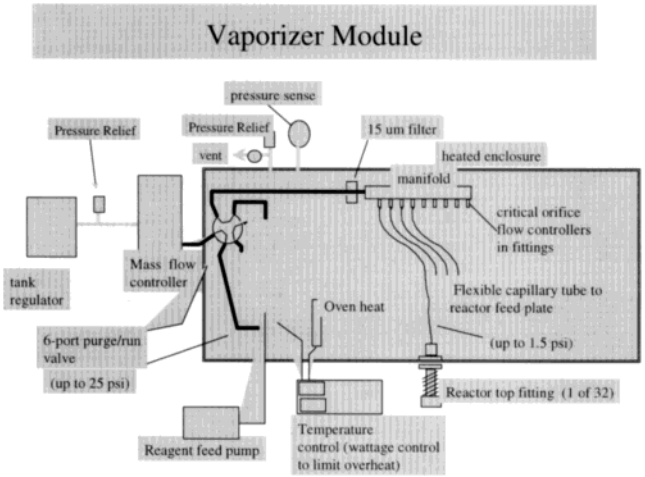

Figure 3. Vaporizer module.

weight difference in the SiO_2 bed before and after reaction was also determined; however, a black carbon-based deposit rendered a precise weight determination impossible.

The following SiO_2 sources were used initially in the described procedure: silica gel [Davison Chemical Division W. R. Grace & Co (grade 12; 700 m^2/g surface area)]; natural diatomaceous earth (Celite Snow Floss, Celite 209, Celite FC, and Dicalite SA-3); calcined diatomaceous earth (Celite 270); flux-calcined diatomaceous earth (Celite Hyflo and Celite 545).

A large number of mineral and rock sources were obtained as described in the body of the text. Minerals were crushed in a Denver Equipment Co. jaw crusher and then ground in a SPEX Industries shatterbox. The list of all materials investigated and their origin can be found in the Supporting Information.

High Throughput Screening. A 32 tube reactor system was employed. The reactor had a region to supply or generate a reacting vapor, gas flow control to a parallel array of replaceable reactor tubes, temperature control of the reactor tubes, and a region where the reacted streams flowed from the reactor tubes to collecting vials for later analysis. A block diagram of the reactor is shown in Figure 2.

As shown in Figure 3, the mixing chamber was heated and purged with a controlled flow of carrier gas while DMC was added at a controlled rate to give a reactant gas mixture of known composition.

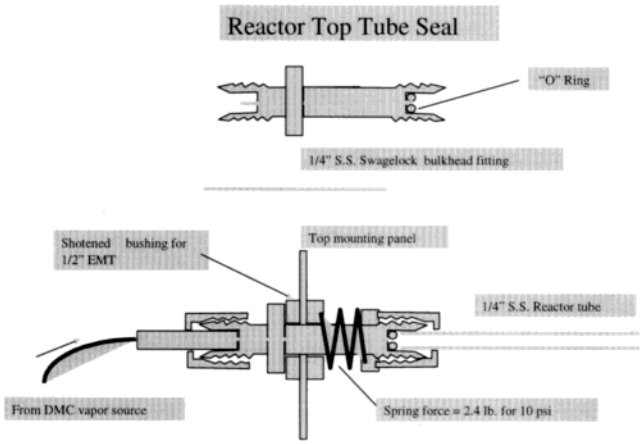

Figure 4. Example of spring-loaded reactor end seals.

The reactant gas mixture generated by the vaporizer was then fed to a manifold to distribute the reactants to the array of reaction tubes. The manifold and flow lines were maintained at elevated temperature to avoid condensation of DMC from the gas stream. To obtain meaningful comparisons of activity of the condensed phase reagent with the DMC, the flow rate of the vapor was controlled to provide similar gas flow rates through each reaction tube. Capillary tube restrictors were employed as passive flow control devices for distribution to the array of reaction tubes.

We utilized elastomer or inert thermally stable polymer seals to provide a gastight seal at the entrance and exit of the reactor tubes (Figure 4). The reactor tube length was substantially longer than the heater block to permit cooling of the exposed portions of the tubes and thus reduced thermal effects on the elastomer seals. The seals at the bottom end of the reaction tube are spring loaded and allowed to move in the reaction tube axis while mounted on a locating plate.

The exit gases from the reactor tubes were passed through a bundle of 32 heated capillary tubes to an array of 32 culture tubes containing dichlorobenzene in a cooled block.

High-Speed Gas Chromatography. Gas chromatographic analysis was carried out using the EZ-Flash GC accessory from Thermedics. The EZ-Flash is an accessory for conventional gas chromatographs that directly heats the capillary column permitting very high heating rates and temperature uniformity. The fundamental separating capability of the column was maintained while dramatically shortening analysis time without a decrease in peak resolution.

The column used for the HTS reactor products was a silicone-coated capillary from Restek (RTX-5). The column was a 5 m 0.25 mm diameter capillary coated with 0.5 μm of a cross-linked dimethylsiloxane. The EZ-Flash temperature program consisted of a hold for 30 s at 40 °C followed by a ramp to 280 °C at 60 s (480 °C/min) and a 15 s hold at 280 °C. The carrier gas was helium at 15 psi head pressure, the injector and flame detector temperatures were 290 °C, and a 1 μL injection was used in split mode with a split ratio of 120:1. The oven program on the host HP5890-II GC was as follows: a 30 s hold at 40 °C, then a ramp at 10 °C/min to 41 °C, followed by a ramp at −40 °C/min to 40 °C, and a hold for 22 s. The short temperature program avoided HP fault shutdown due to oven temperature excursions and permitted rapid cooling of the EZ-Flash column to the start condition.

XRD. X-ray diffraction was performed on 37 mineral samples in an effort to identify individual phases in each of the samples. A majority of the samples (29 samples) were measured on a Siemans D500 diffractometer, which utilizes a Bragg−Brentano vertical

Θ−2Θ goniometer geometry, while the remainders (8 samples) were measured on a Scintag XDS 2000 diffractometer, utilizing a Bragg−Brentano vertical Θ−Θ goniometer geometry.

Both instruments used a Cu anode tube (wavelength for Cu Kα1 = 1.54056 Å), and samples were typically measured at the following parameters:

power generation	instrument setup
kV = 45	2θ range = 10−90°
mA = 40	step size = 0.05°
	dwell time = 2 s
	slit sizes:
	Siemans D500 = 1°
	Scintag XDS 2000 = 0.5/0.3

Variations in the setup were typically due to analyses specific to a certain sample (e.g., placing tape over the surface of certain samples in an effort to maintain optimal measuring surface, extending the 2θ range to explore additional peaks in a sample, etc.). All samples were top-loaded into an Al cavity mount sample holder.

Upon the completion of each measurement, the spectra were then analyzed with Materials Data, Inc. (MDI) Jade XRD pattern processing software package (version 5.0.24). Using information such as chemical composition, 2θ/d-space position, and peak intensity, all phases were referenced to the International Centre for Diffraction Data (release 1999) database[16] for the closest reasonable match. Determination of mineral phases was sometimes supported by knowing the likely appearances of certain minerals with each other.[17]

Procedure for Analyzing Powder Using Image Analysis. Small samplings of powder were removed and placed on a glass slide. A small droplet of dispersion fluid with a refractive index that provided good contrast between the powder and background was applied to a glass cover slip. The cover slip was placed on the powder sample and dispersed using mechanical agitation. The slide was then placed on a transmitted light microscope (Zeiss Photomicroscope III) and observed at sufficient magnification to distinguish the size and shape of the powder. The microscope was outfitted with a high-resolution camera (Kodak ES1) that was interfaced to a computer in order to provide a digital image for further analysis. Image analysis software (Clemex Vision) was used to quantify the particle sizes.

Three samplings of powder were taken from each vial and analyzed. Three areas were imaged from each slide for a total of at least nine areas measured for analysis. This procedure provided good statistical sampling (95% confidence limits) of the true particle size distribution of the powder. The size distribution was displayed in two forms: number and volume. The size distribution based on number was created by determining the number of particles that fell between size ranges. The size distribution based on volume was made with the assumption that each particle approximated a sphere. In this way, each particle diameter was transformed into a volume using standard formulas, and the distribution was based on the number of particles that fall between volume ranges (expressed as diameter). The importance of these two distributions lies in the fact that very often a plethora of very small particles were present that did not account for all of the volume. Using both forms illuminated the true distribution character of the powder.

(16) Powder Diffraction File, Release 1999, Data Sets 1−49 plus 70−86 PDF; ISSN 1084-3116; International Centre for Diffraction Data, 12 Campus Boulevard, Newtown Square, PA 19073-3273. Internet: information@icdd.com, www.icdd.com.

(17) *The Audubon Society Field Guide to North American Rocks and Mineral*, 10th printing; Alfred A. Knopf, Inc.: New York, 1990.

Table 1. Ranges of Selected Properties of Diatomaceous Earth Products[a]

property	natural	calcined	flux-calcined
specific gravity	2.00	2.25	2.33
porosity, by volume (%)	65−85	65−85	65−85
surface area (m^2/g)	10−30	4−6	1−4
crystalline content (%)	<5	5−10	>60

[a] Values given are typical or estimated values from product literature.

Results and Discussion

Validation of Literature Synthesis of Q′. The reported base-catalyzed synthesis of Q′ starting from silica gel[5] was investigated serving two purposes, first to test this reaction in our reactor setup and second to use the data as a benchmark for other SiO_2 sources. The literature procedure used a small-scale setup (2 mmol, 120 mg of SiO_2), and the reactor downstream was directly monitored by GC without the use of a condenser. Quantitative SiO_2 utilization was reported.[5]

Silica gel (200 mg), loaded with 4.5% KOH catalyst, was reacted with DMC at 320 °C. GC analysis of the liquid obtained downstream showed only two signals, Q′ and unreacted DMC. SiO_2 utilizations of 93% and 88% were found for two independent experiments. The SiO_2 beds turned deep black indicating carbon deposition. Presumably, a competing, nonproductive decomposition of DMC C−H bonds occurs which leads to carbon deposition.

Q′ from Silica Gel. In the context of screening available SiO_2 sources, silica gel was used as a reagent. The silica gel, doped with 4.6% KOH, reacted almost quantitatively with DMC at 320 °C. Silica gel reactivity was used as the standard against which all other silicon dioxide sources were measured.

Diatomaceous Earth, a Low-Cost SiO_2 Source. The literature synthesis of Q′ used silica gel as the SiO_2 form; silica gel is commercially unattractive. Additionally, silica gel has a very high surface area (>100 m^2/g). The biggest challenge for potential commercial implementation of the base-catalyzed synthesis of Q′ from SiO_2 and DMC represented the discovery of reactivity using a low-cost silicon dioxide source.

Diatomaceous earth (DE), also known as diatomite, is a naturally occurring, porous, high surface area form of hydrous silica. DE consists mainly of accumulated shells of intricately structured amorphous hydrous silica secreted by diatoms, which are microscopic, single-celled algae. All diatom species (more than 12000 species are known) have an elaborately ornamented siliceous skeleton, which results in accumulations of uniquely porous particle of high surface area. Three general types of DE are commercially available, natural, calcined, and flux-calcined. The natural product results from mining of the crude DE, careful grinding (to preserve the intricate structure of DE), and drying. The calcined type is produced by subjecting the natural DE to high temperatures (900−1000 °C). The flux-calcined material is obtained by calcining the natural product in the presence of a fluxing agent, generally sodium carbonate. A selection of relevant properties is listed in Table 1. Annual production in 1990 in the USA totaled 619000 t and exceeded 1.8 Mt worldwide.

Figure 5. SEM of natural DE (Celite Snow Floss).

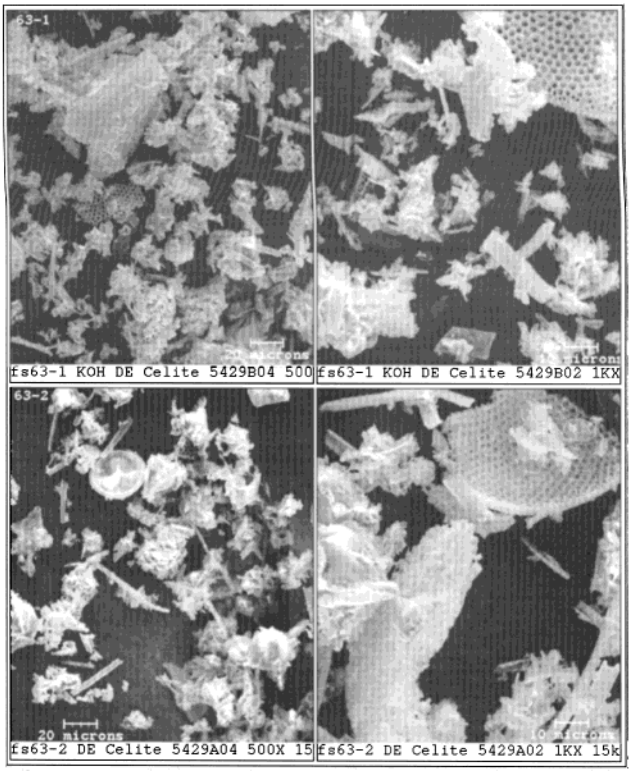

Figure 6. SEM of flux-calcinated DE (Celite Hyflo) with KOH (top) and without KOH (bottom).

SEM Analysis of DE Samples. SEM surface analysis was carried out on Celite Snow Floss (natural DE) with and without KOH catalyst (Figure 5) and on Celite Hyflo (flux-calcined DE) with and without KOH catalyst (Figure 6). Figures 5 and 6 showed the intricate structures of various DE species. The natural DE sample exhibited a wide distribution of particle sizes. In comparison, the flux-calcined DE had a lower particle size distribution and also showed some flake type materials.

As a result of its natural formation, DE contains a wide variety of metals in the form of their oxides in addition to SiO_2. SiO_2 contents range between 70% and more than 90%. Most of the samples commercially available in the U.S. contain 85%−90% SiO_2. For example, Celite Hyflo contained Al (2.6%), Fe (1.0%), Na (3.3%), K (0.5%), Ca (0.4%), Mg (0.4%), Ti (0.1%), and other elements (50−1000 ppm) such as Ba, Mn, Ni, Cr, Zn, and Sr.

SiO_2 Utilization. DE, treated with KOH, reacted at temperatures between 300 and 360 °C to yield Q′. The SiO_2 utilization was a function of the commercial grade of the DE. The flux-calcined grade (Celite Hyflo) exhibited the lowest SiO_2 utilization (<5%). SiO_2 utilization for the calcined grade was 10% (Celite 270). SiO_2 utilization for the natural grade DE (Celite Snow Floss) was optimized to >60%. The difference in reactivity between the three commercially available grades could best be explained by the variation in surface area, crystallinity, and porosity (Table 1), with the surface area most likely representing the decisive factor (higher surface area equals higher SiO_2 utilization).

The SiO_2 utilization also depended on a variety of process factors; the most vital were the amount of KOH loading and the reaction temperature.

DMC Decomposition. The decomposition of DMC into dimethyl ether and carbon dioxide was already reported as a significant side reaction in the work by Ono et al.[4] At 277 °C, Ono and co-workers found the DMC consumption and the transformation of DMC into Q′ to be about equal, indicating that the gas-phase decomposition of DMC was negligible. However, at 327 °C, they reported significant decomposition.

Our mass balance analysis supported the Ono findings. DMC utilization is defined as the ratio of DMC reacted toward Q′ and the DMC consumed. DMC consumed was calculated by subtracting the recovered DMC from the added DMC. It was important to note that DMC loss due to inefficient trapping by the condenser was included. Typically, DMC utilization for the commercially viable natural DE was less than 20%.

Mechanistic Aspects. A plausible mechanism is depicted in Figure 7. The mechanism is consistent with the data reported by Ono et al., computational data from Molecular Simulations Inc.,[18] and our own observations.

Consistent with the literature,[19] the KOH-treated SiO_2 surface likely contains Si−O−K linkages as structural units under the typical reaction conditions. Calculations by Molecular Simulations Inc. (MSI) (by L. Subramanian using Dmol^3)[18] showed that Si−O bonds elongate upon interaction with the potassium ion (from 1.63 to 1.67 Å), suggesting an

(18) (a) Wimmer, E. *NATO Adv. Study Inst. Ser., Ser. C* **1997**, *498*, 195. (b) Spiess, L.; Wimmer, E.; Soukiassian, P. *Appl. Surf. Sci.* **1996**, *92*, 501−6.

(19) Iler, R. K. *The Chemistry of Silica*; John Wiley and Sons: New York, 1979.

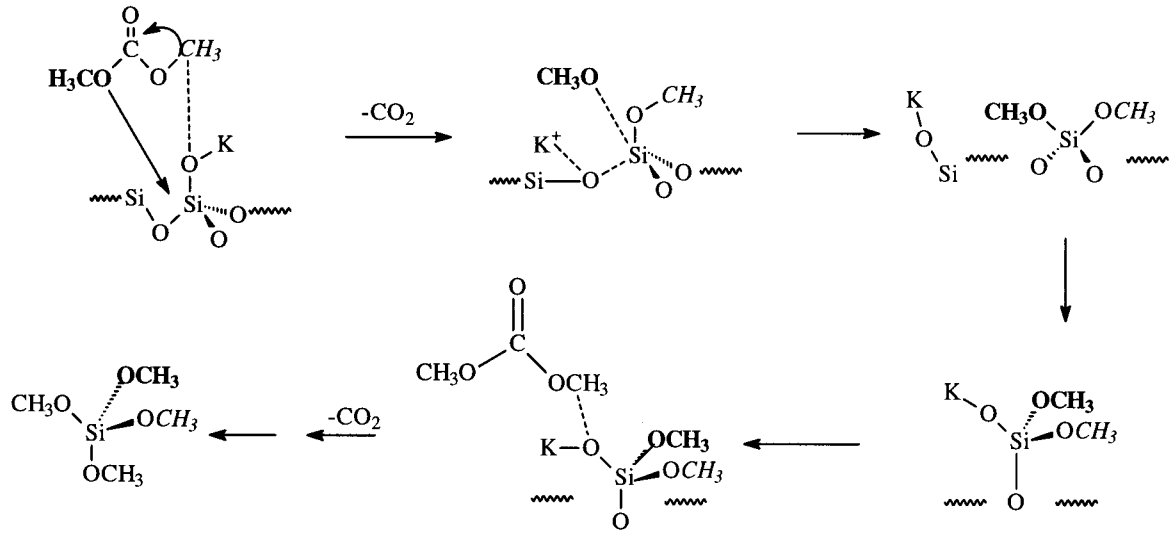

Figure 7. Proposed mechanism for the base-catalyzed formation of Q′ from SiO_2.

activation of the Si−O bond. Experiments using a modified reactor setup that allowed mass spectrometry detection directly downstream of the reactor showed the exclusive production of CO_2 directly after the start of the DMC addition. Q′ formation was observed after a delay consistent with the proposed mechanism because initially the reaction of DMC with the potassium-containing SiO_2 surface resulted solely in the methoxylation of the silica surface under formation of CO_2 (Figure 7). The formation of Q′ requires a second activation of the methylated silica surface by K^+ followed by reaction with a second molecule of DMC. The proposal in Figure 7 is also consistent with base-mediated reaction of SiO_2 with ethylene glycol as reported.[10]

Silicate Minerals. Given the exciting lead provided by diatomaceous earth, a screen of silicate minerals was suggested. Well over 200 silicate minerals were screened for their reactivity with DMC and base. All of these minerals were crushed, ground, sieved, premixed with aqueous base, dried, and then reacted with DMC. High-speed gas chromatographic (GC) analysis (EZ-Flash) permitted rapid analysis of the products. The amount of Q′ formation was compared to a reaction internal standard for each experiment. Not all of the minerals gave silicon-containing volatile products, however; the only product ever observed was Q′. The most promising silicate candidates, in terms of Q′ yield, were reacted in the traditional "one-at-a-time" mode using the fixed bed reactor with a larger bed volume. Attempts were also made to analyze and determine the precise nature of the promising minerals found in the screen.

The HTS reactor permitted 32 simultaneous fixed bed experiments to be performed. An LC pump was used to pass liquid reagent (DMC) through a vaporizer so that the reagent could be delivered to the reactor as a gas. Each tube was loaded with a previously ground mineral, premixed with 5%−10% base (usually KOH). Unreacted DMC, other by-products, and product (if any) passed through heated transfer lines and condensed into tubes containing *o*-dichlorobenzene with cyclooctane as an internal standard. The mixtures were analyzed by high-speed gas chromatography. It was well

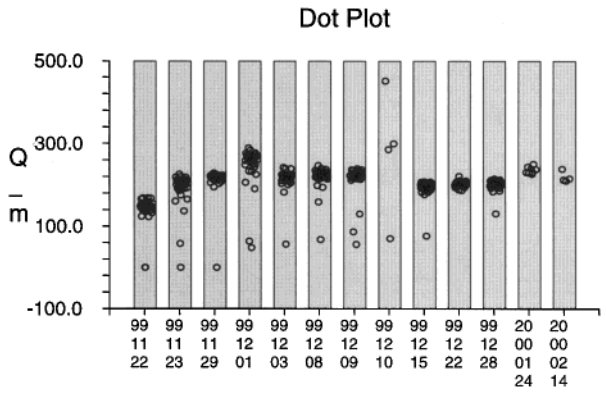

Figure 8. Reproducibility study of formation of Q′ from silica gel (5% KOH) in the 32 column reactor. Plot of grams Q′/grams of SiO_2 charge vs number of trials.

established in the single tube reactor that silica gel and 5% KOH reacted with DMC at 350 °C to give Q′ (vide supra). In a series of reactor runs, up to 32 tubes were loaded with silica gel containing 5% KOH from a master batch. The reproducibility of formation of Q′ within and between runs is shown in Figure 8, where m = the initial charge of SiO_2. These experiments showed that a Q′/m difference of ∼30 can be determined with 95% confidence.

Mineral samples for study were obtained from a variety of sources. The silicates are classified into seven structural forms.[20] As shown, there was no clear correlation between a particular mineral class and the propensity to form Q′.

Over 200 different minerals were screened for reactivity with DMC in the presence of base. In every 32 column block of samples reacted, quadruplicates of the silicate were run as well as quadruplicates of silica gel and quadruplicates of sea sand. The sea sand (despite the fact that we call this project "Sand to Silicones") was nominally a low value in our experiments. Thus, in every 32 column run, we had an internal check to ensure that Q′ was produced and that it was compared to our low value. GC integrator area % values

(20) Klein, C.; Hurlbut, C. S. *Manual of Mineralogy*, 21st ed.; John Wiley & Sons: New York, 1993; pp 442−3.

Table 2. Most Active Minerals for Formation of Q′ from Reaction with DMC and Base

mineral	formula	structure	Q′/sand	size (vol)	size (#)
opal	SiO_2	tectosilicate	102.8	15	6.15
opal	SiO_2	tectosilicate	85.4	1.5	1.13
Celite Sno Floss	SiO_2	tectosilicate	68.5	1.74	1.4
Celite 209	SiO_2	tectosilicate	30.9	23.4	12.37
flint clay	$Al_2O_3-SiO_2$	tectosilicate	29.7	26.2	16.5
shattuckite	$Cu_5(SiO_3)_4(OH)_2$	Inosilicate	26		
Celite FC	SiO_2	tectosilicate	19	5	3.25
Co ortho silicate	Co_2SiO_4		15.1	4.4	3.09
allophane	$Al_2O_3{\cdot}(SiO_2)_{1.3}{\cdot}2.5(H_2O)$	phyllosilicate	14	9.8	5.91
tuff	SiO_2	tectosilicate	10.5	14.6	6.37
shale ferruginous			9.9	12.8	7.49
serpentine	$Mg_3Si_2O_5(OH)_4$	phyllosilicate	9.6	9.2	4.9
Ca ortho silicate meta wollastonite	$CaOSiO_2$		9	10.1	78.6
sugilite	$(Na,K)AlSiO_4$	tectosilicate	8.9	24.3	10.5
Li meta silicate	Li_2SiO_3		8.7	14.3	7.4
gem silica	SiO_2		7.4	22.8	10.1
amosite	$(Fe,Mg)_7Si_8O_{22}(OH)_2$	inosilicate	7.3		
pyrophyllite	$Al_2Si_4O_{10}(OH)_2$	phyllosilicate	7.3	49	41.6
Celite HyFlo	SiO_2	tectosilicate	7.1	15	8
garnet	33% SiO_2	neosilicate	7	4.7	2.95
mica	$K_2O(Al_2O_3)_x(SiO_2)_y$	phyllosilicate	6.8	8.8	3.8
heulandite C	$CaAl_2Si_7O_{18}{\cdot}6H_2O$	tectosilicate	6.6	14.1	7.85
heulandite B	$CaAl_2Si_7O_{18}{\cdot}6H_2O$	tectosilicate	6.2	23.7	9.9
sugilite	$(Na,K)AlSiO_4$	tectosilicate	6.1	314	59.6
shale carbonaceous			6.1	10.9	6.6
clay	MV, North Shore		6.1	3.5	2.5
schist albite	$(NaAlSi_3O_8)_x(CaAl_2Si_2O_8)_y$	tectosilicate	6.1	44.1	21.1
andalusite	Al_2SiO_5	neosilicate	6	36.1	15.1
Celite 545	SiO_2	tectosilicate	6	12.1	9.9
shattuckite	$Cu_5(SiO_3)_4(OH)_2$	inosilicate	4.9	13.8	5.8
orthoclase	$KAlSi_3O_8$	tectosilicate	4.8	86.2	53.3
ilvaite	$Ca(Fe^{2+})_3(Fe^{3+})O(Si_2O_7)(OH)$	sorosilicate	4.5	59	19
zircon	$ZrSiO_4$	neosilicate	4.2	1.8	1.36
jade	$Ca_2Mg_5Si_8O_{22}(OH)_2$	inosilicate	4.2	14.1	5.88
slate			4	8	4.32
lazurite	$(Na,Ca)_8(AlSiO_4)_6(SO_4,S,Cl)_2$	tectosilicate	3.8	10.9	6.39

for Q′ formed from sand were usually around 4−5, and values for the minerals in Figure 9 ranged from over 600 area units to around 30 with a standard deviation of 3 units. Figure 9 shows the major "hits" from the screen. The amount (in milligrams) of Q′ formed was compared to that produced from sand from each 32 column run. Figure 9 gives a graphical representation of the activity of all the minerals used in the combinatorial screen.

As was found previously, the diatomaceous earth materials were quite reactive with DMC in the presence of base to form Q′. Other amorphous materials were reactive as well, most notably opal. Three synthetic silicates of Co, Li, and Ca were also found to be reactive with base and DMC to form Q′. We initially anticipated that the presence (or absence) of certain metals would be important, and further, we wondered if the particle size of the ground mineral powders would also be important. No correlation could be found between particle size or elemental composition in terms of the propensity of a mineral to react with base and DMC to give Q′. The most important attribute for the reactivity of interest was crystallinity of the silica phase; namely, amorphous materials had the highest reactivity.

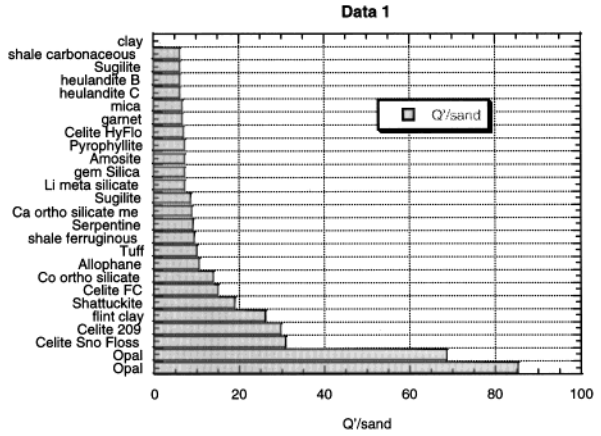

Figure 9. Reaction of minerals with DMC and base to form Q′, best performers.

Single Reactor Experiments. Preliminary work showed that the amorphous diatomaceous earth materials were the most active for formation of Q′. Additionally the flux-calcined diatomaceous earth powders had significant crystalline components. Flux-calcined Celites reacted poorly with base and DMC to give Q′. Using the results from the high throughput screen, we ran the "hits" in a larger scale, one-at-a-time reactor. The results of the single experiment runs are shown in Table 2. This table also shows the number average and volume average particle size for each material in the table. The particle size data were obtained by image analysis.

The results from the high throughput screen showed that reaction of opal and base with DMC gave the highest yields of Q′. Thus, the opal reaction was used to determine the repeatability of using the fixed bed reaction. Six replicate experiments were run in the fixed bed where opal with 5%

KOH was reacted with DMC at 350 °C. About 20% yield of Q′ was obtained with a standard deviation of 3%.

DMC decomposition also occurred in the course of the reaction of silicate/base with DMC. DMC utilization was 58% with a standard deviation of 20% for six replicate runs. Obviously, the utilization of DMC was neither highly optimized nor very reproducible.

Mineral Analysis. Unlike a traditional chemistry experiment, experiments performed with rocks or minerals have the problem that the "reagent" may not be pure or may be poorly characterized (caveat emptor!). Some of the minerals used in the combinatorial screen were analyzed by X-ray diffraction (XRD) and by X-ray fluorescence (XRF). The diffraction pattern for most common minerals is well-known, and so, XRD patterns for pure materials should match literature patterns. In many cases, two or more components were present in our samples, and so, the observed patterns were composed of components of the mixture. As a result of our screening experiments, we found that our best performing materials were amorphous silicates. XRD measurement on amorphous materials will usually give just broad patterns. A table of the results of the XRD screen is given in the Supporting Information. Figure 10 gives a representative example of the observed XRD pattern for a material and the match of that pattern to a known material. Additional patterns are provided in the Supporting Information section.

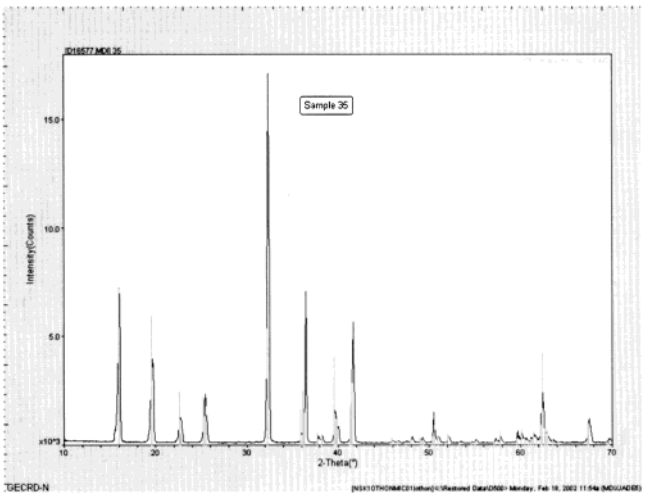

Figure 10. XRD pattern for andalusite; (Al_2SiO_5); excellent match with PDF No. 39-376.

Conclusions

Crystalline samples for the most part were unreactive toward formation of Q′. The amorphous materials such as the natural Celite, opal, and Co, Li, and Ca silicate gave the best results. Note that the flux-calcined Celite had a significant crystalline component. Some materials were not at all what we thought they were, such as most of the heulandite, one of the sugilites, and the allophane. Surprisingly, shale found on the GE CRD grounds and a clay sample from Martha's Vineyard's north shore had nearly identical XRD patterns. As previously reported,[6] rice-hull ash is a low cost form of silicon dioxide useful for production of Q′. This study identified diatomaceous earth as another low-cost source of silicon dioxide for the Q′ process. Opal is expensive in the gem form, but opal tailings are available at reasonable cost and represent another low-cost silicon dioxide source.

Acknowledgment. All the work described in this report would have not been possible without the help of many people. We thank Ted Sun and Stan Stoklosa for the preparation of the sol-gel materials and Molecular Simulations Inc. for the calculations. John Leman has been an invaluable pool of information. We thank Woody Ligon and Hans Grade for the GC/MS work and the fast turnaround times and June W. Klimash and Nancy Marotta for the elemental analysis.

Supporting Information Available: Additional tables and figures. This material is available free of charge via the Internet at http://pubs.acs.org.

IC0109546